2006

The effect of oxidation on the structure of styryl-substituted sexithiophenes: A resonance Raman spectroscopy and density functional theory study

Tracy Clarke
University of Otago

Keith Gordon
University of Otago

David L. Officer
University of Wollongong, davido@uow.edu.au

Daina K. Grant
Massey University

The effect of oxidation on the structure of styryl-substituted sexithiophenes: A resonance Raman spectroscopy and density functional theory study

Abstract

The structures and vibrational properties of a series of styryl-substituted sexithiophenes and their charged species have been examined using resonance Raman spectroscopy in conjunction with density functional theory calculations. The calculated geometries of the radical cations and dications indicate that the quinoidal charged defects are more strongly localized in the center of the thiophene backbone than is observed in other sexithiophenes. This defect confinement, induced by the positions of the styryl substituents, is particularly evident in the dication species. However, the defect confinement weakens when alkoxy groups are added onto the phenyl rings by causing the extension of the charged defect into the styryl groups. The Raman spectra of the neutral styryl sexithiophenes are dominated by intense thiophene symmetrical stretching modes in both the measured and predicted spectra.Oxidation generates radical cations and dications, both of which can be observed in the solution state resonance Raman spectra. Unlike other sexithiophenes, which generally show a downshift of the intense thiophene stretching mode from the radical cation to the dication, a small upshift is observed for the styryl-substituted sexithiophenes. The theoretical spectra predict an insignificant change during this transition and the eigenvector for this mode reveals that it is localized over the same area occupied by the confined defect. In contrast, the solid state resonance Raman spectra of electrochemically oxidizedfilms reveal evidence of solely radical cations and there is an appreciable downshift of the intense thiophene stretching mode compared with the corresponding mode in the solutionspectra. This implies that the increase in the effective conjugation length from the solution to the solid state is greater for the radical cations than for the neutral species. It therefore appears that the radical cations form π stacks in the solidfilm and the resulting intermolecular interactions effectively allow a further extension of the electron delocalization.

Keywords

oxidation, structure, styryl, effect, sexithiophenes, study, raman, density, functional, theory, substituted, resonance, spectroscopy

Disciplines

Engineering | Physical Sciences and Mathematics

Publication Details

Clarke, T. M., Gordon, K. C., Officer, D. L. & Grant, D. K. (2006). The effect of oxidation on the structure of styryl-substituted sexithiophenes: A resonance Raman spectroscopy and density functional theory study. Journal of Chemical Physics, 124 (16), 164501-1-164501-11.

The effect of oxidation on the structure of styryl-substituted sexithiophenes: A resonance Raman spectroscopy and density functional theory study

Tracey M. Clarke, Keith C. Gordon, David L. Officer, and Daina K. Grant

Citation: The Journal of Chemical Physics **124**, 164501 (2006); doi: 10.1063/1.2185095
View online: http://dx.doi.org/10.1063/1.2185095
View Table of Contents: http://scitation.aip.org/content/aip/journal/jcp/124/16?ver=pdfcov
Published by the AIP Publishing

The effect of oxidation on the structure of styryl-substituted sexithiophenes: A resonance Raman spectroscopy and density functional theory study

Tracey M. Clarke and Keith C. Gordon[a)]
Department of Chemistry and MacDiarmid Institute for Advanced Materials and Nanotechnology, University of Otago, P.O. Box 56, Dunedin, New Zealand

David L. Officer
Nanomaterials Research Centre and MacDiarmid Institute for Advanced Materials and Nanotechnology, Massey University, Private Bag 11222, Palmerston North, New Zealand

Daina K. Grant
Nanomaterials Research Centre and MacDiarmid Institute for Advanced Materials and Nanotechnology, Massey University, Private Bag 11222, Palmerston North, New Zealand and New Zealand Institute for Crop & Food Research Ltd., Private Bag 11600, Palmerston North, New Zealand

(Received 3 November 2005; accepted 14 February 2006; published online 24 April 2006)

The structures and vibrational properties of a series of styryl-substituted sexithiophenes and their charged species have been examined using resonance Raman spectroscopy in conjunction with density functional theory calculations. The calculated geometries of the radical cations and dications indicate that the quinoidal charged defects are more strongly localized in the center of the thiophene backbone than is observed in other sexithiophenes. This defect confinement, induced by the positions of the styryl substituents, is particularly evident in the dication species. However, the defect confinement weakens when alkoxy groups are added onto the phenyl rings by causing the extension of the charged defect into the styryl groups. The Raman spectra of the neutral styryl sexithiophenes are dominated by intense thiophene symmetrical stretching modes in both the measured and predicted spectra. Oxidation generates radical cations and dications, both of which can be observed in the solution state resonance Raman spectra. Unlike other sexithiophenes, which generally show a downshift of the intense thiophene stretching mode from the radical cation to the dication, a small upshift is observed for the styryl-substituted sexithiophenes. The theoretical spectra predict an insignificant change during this transition and the eigenvector for this mode reveals that it is localized over the same area occupied by the confined defect. In contrast, the solid state resonance Raman spectra of electrochemically oxidized films reveal evidence of solely radical cations and there is an appreciable downshift of the intense thiophene stretching mode compared with the corresponding mode in the solution spectra. This implies that the increase in the effective conjugation length from the solution to the solid state is greater for the radical cations than for the neutral species. It therefore appears that the radical cations form π stacks in the solid film and the resulting intermolecular interactions effectively allow a further extension of the electron delocalization. © *2006 American Institute of Physics*. [DOI: 10.1063/1.2185095]

INTRODUCTION

Polythiophenes are a class of π-conjugated polymers that have received considerable attention in recent years due to their potential use in plastic electronics applications such as photovoltaic devices.[1] However, such polymers also possess a number of disadvantages, including insolubility and polydispersity, which make them difficult to study. Oligothiophenes, on the other hand, have greater solubility and can be well defined in their chemical and physical properties.[2–4] Indeed, efficient thin film transistor devices based on oligothiophenes, sexithiophene in particular, have been reported.[5]

One aspect of this class of materials is their ability to conduct charge in the oxidized (doped) state. However, the precise mechanism of conduction is still under debate, in particular, the identity of the primary charge carrier. In the case of polythiophene, a nondegenerate polymer, oxidation produces polarons (radical cations) and bipolarons (dications), both of which are potential charge carriers.[6] These species are defined as both the charged excitation and the structural defect that it induces. These charged defects, characterized by a domain of quinoidal bond sequence, are localized over several monomer units. Theoretical works (*ab initio* and semiempirical) on oligothiophenes have demonstrated that polarons extend over approximately three or four[7] thiophene rings while bipolarons extend over six[8] to nine[9,10] rings (depending on the definition of the defect boundaries).

Vibrational spectroscopies (Raman and infrared) have often been used to examine the structural properties of oligothiophenes and their radical cations and dications. Reso-

[a)]Author to whom correspondence should be addressed. Electronic mail: kgordon@alkali.otago.ac.nz

nance Raman spectroscopy, in particular, is a suitable experimental technique for the investigation of these charged species. Excitation wavelengths are chosen specifically to coincide with the electronic absorption bands of the particular species that requires study: the intensities of the symmetrical vibrational modes belonging to this species are preferentially enhanced. Density functional theory (DFT) calculations have proven a useful tool to aid in the analysis of the resultant vibrational spectra in terms of the nature of the modes and the degree of structural change between the neutral and charged species. The vibrational spectra of various oligothiophene radical cations and dications have been studied in this manner;[2,8,11–13] the most comprehensive of which are a series of thiophene-based oligomers containing ethenyl linkages[4,14] and a variety of alkyl end-capped oligothiophenes.[7,15] These studies have shown the expected development of quinoidal structure along the thiophene backbone of the charged species and the reflection of this structural change in the vibrational spectra. The transition from an aromatic to quinoid bond sequence upon creation of a radical cation or dication has been predicted by *ab initio* calculations and also observed experimentally as a downshift of an intense band due to a CC stretching mode of the oligothiophene backbone.[2,7,8,16] In addition, information on the chain length dependence and substitutional effects has been provided by these investigations.

The neutral molecules of a series of substituted terthiophenes, 3′-[1*E*-2-(4-*R*-phenyl)ethenyl]-2,2′:5′,2″-terthiophene, where *R* differs in its electron-donating capacity, have previously been investigated.[17] The calculated vibrational spectra of this *R*-pet series correlate well to the experimental spectra, allowing information on their geometries to be established. The electrochemical and electronic absorption properties of these compounds and a number of related alkoxy-styryl-substituted terthiophenes and sexithiophenes have also been examined.[18] All of these styryl-terthiophenes σ dimerized to form sexithiophenes upon oxidation, and evidence of sexithiophene radical cations, π dimers, and dications were obtained from the electronic absorption spectra.

This paper presents the vibrational spectral data and calculated structures of the styryl-substituted sexithiophenes and their charged species. We find that the polaron and bipolaron structures are strongly confined in the center of the thiophene chain between the β-styryl substituents. This defect confinement is significantly more pronounced than in other sexithiophenes and it may explain the lack of further polymerization in these styryl-substituted sexithiophenes.[19]

EXPERIMENT

The chemical structures of the compounds studied are shown in Fig. 1. The synthesis of these compounds has been described elsewhere.[19,20] Chemical oxidations were performed using 1.0×10^{-5}–2.0×10^{-3} mol L^{-1} oligothiophene solutions, prepared with spectrophotometric grade acetonitrile. Oxidant, a solution of 10^{-4}–0.1 mol L^{-1} copper perchlorate in acetonitrile [$Cu(ClO_4)_2/CH_3CN$], was added until the desired oxidation product was reached. Raman spectra

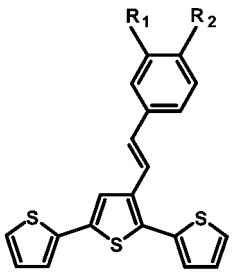

I: R_1 = -H, R_2 = -H
II: R_1 = -H, R_2 = -OCH_3
III: R_1 = -OCH_3, R_2 = -OCH_3
V: R_1 = -OCH_3, R_2 = -$O(C_2H_4O)_3CH_3$
VII: R_1 = -H, R_2 = CN

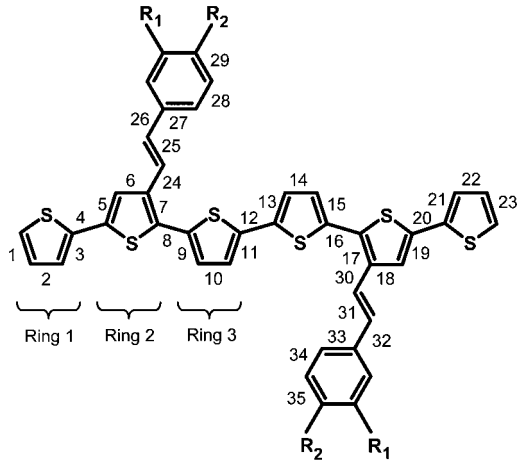

IV: R_1 = -OCH_3, R_2 = -OCH_3
VI: R_1 = -OCH_3, R_2 = -$O(C_2H_4O)_3CH_3$

FIG. 1. The chemical structures of the compounds studied and the bond numbering system used for the styryl sexithiophenes.

of the oxidized solutions were measured with an excitation wavelength of 752 nm using a system described previously, except that a 50 μm entrance slit to the spectrograph was used.[21]

Solid films of the oxidized species were produced electrochemically on an indium tin oxide (ITO) glass immersed in an oligothiophene solution by applying an oxidizing potential (0.9–1.2 V) using deposition times of 2–10 min. The auxiliary electrode was a platinum mesh and a Ag/AgCl reference electrode was used. Films of the neutral sexithiophenes were generated from the terthiophenes by applying a reducing potential of 0 V after the initial oxidation deposition. Raman spectra of the oxidized films were measured using 752 nm excitation and the neutral films were measured using 413 nm excitation. These excitation wavelengths were chosen to provide resonance with the oxidized and neutral sexithiophenes, respectively.[18]

Fourier transform (FT) Raman spectra of the neutral oligothiophenes were recorded from solid powder samples using a Bruker IFS-55 FT-interferometer bench equipped with an FRA/106 Raman accessory and a Ge D425 detector. Radiation of 1064 nm from a Nd:YAG (yttrium aluminum gar-

net) laser with an operating power of 100 mW was utilized for Raman excitation. The FT-Raman spectra were collected after 16–64 scans at a resolution of 4 cm^{-1}. The FT-Raman spectra of the oxidized solutions were also measured.

DFT calculations were carried out using the B3LYP method in conjunction with the 6-31G(*d*) basis set and the GAUSSIAN 03 program.[22] Geometry optimizations of the neutral styryl oligothiophenes and the sexithiophene radical cations and dications were performed using the previous geometry results of the *R*-pet series as a starting point,[17] with the thiophene rings in an all-*anti* configuration. Only the head-to-head regioisomer was calculated. This was followed by a frequency calculation for each species. A scale factor of 0.96 was applied to all predicted frequencies, as previously recommended.[23] It was required that C_2 symmetry be imposed onto the IV and VI systems and their charged species due to the large number of basis functions involved in the calculation. In the case of V and VI, the long chain alkoxy substituent on the phenyl ring was modeled by halving its length. The spin-unrestricted calculation was used for the radical cations (UB3LYP).

RESULTS AND DISCUSSION

Geometry

The first step is to examine the calculated [B3LYP/6-31G(*d*)] geometries of each species and assess the structural changes predicted upon oxidation. A bond length alternation diagram allows these changes to be clearly observed by comparing the CC bond lengths of the neutral and charged species. The geometries of unsubstituted sexithiophene and its charged derivatives have also been calculated for comparison purposes.

In the case of the neutral unsubstituted sexithiophene, an aromatic molecular structure was calculated, as has been predicted for numerous other oligothiophenes[9,24] [Fig. 2(a)]. The sexithiophene radical cation backbone has the expected polaron structural defect in the center of the molecule. The geometry distortion extends over the four central rings, as shown by the reversal of the bond length alternation from an aromatic to a quinoidal pattern. The two terminal rings maintain a full aromatic character. The removal of a second electron to create the dication causes the quinoidal nature of the central four rings to increase significantly and the terminal rings lose their aromatic structure. The two central rings have an average absolute bond length change of 0.045 Å from the neutral species to the dication while the two terminal rings have an average change in bond length of 0.021 Å.

The radical cation and dication structures of the styryl-substituted sexithiophenes also show the formation of a quinoidal bond structure. The bond length alternation diagram of the sexithiophene backbone of $(I)_2$ and its charged species is shown in Fig. 3(a). The central thiophene rings of $(I)_2^{\bullet+}$ have a full quinoid character while the terminal rings

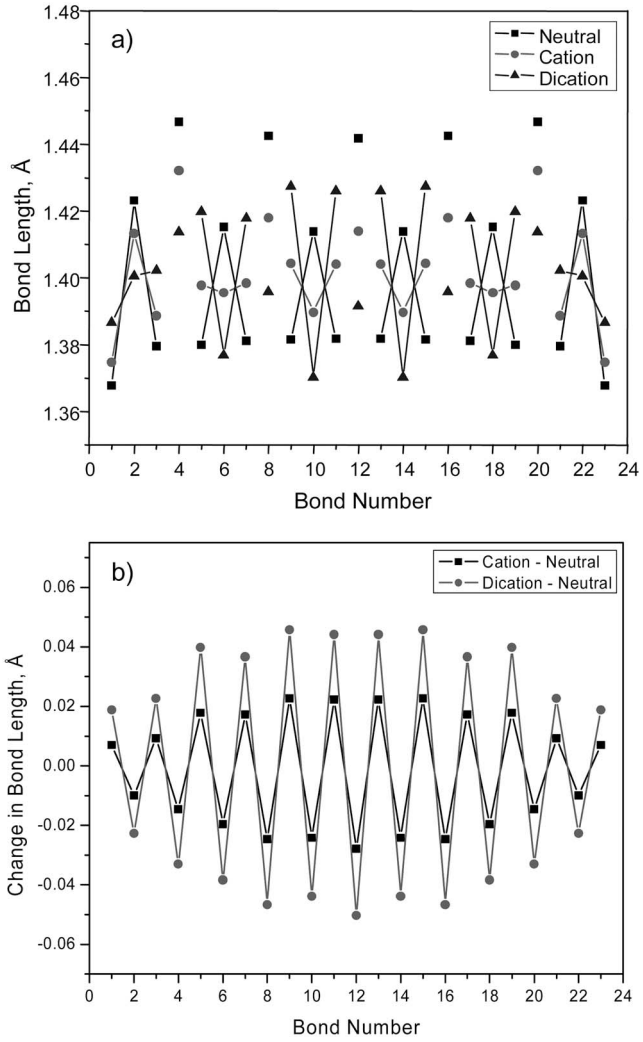

FIG. 2. The calculated [B3LYP/6-31G(*d*)] CC bond length alternation diagram for unsubstituted sexithiophene and its charged species along the sexithiophene backbone (a), using the bond numbering system depicted in Fig. 1. Each set of three connected symbols represents a thiophene ring, while unconnected symbols represent the inter-ring bonds. The change in bond lengths along the sexithiophene backbone between the charged and neutral species (b).

remain aromatic. However, in contrast to the unsubstituted sexithiophene radical cation, the structural defect of $(I)_2^{\bullet+}$ is localized over a smaller area of the thiophene backbone. The charged defect appears to be confined by the styryl substituents in that only the two central rings are fully quinoidal, as opposed to the four central rings observed for unsubstituted sexithiophene. This effect is exacerbated in the case of $(I)_2^{2+}$: the magnitude of the bond length reversal increases considerably for the two central rings. However, the second (bonds 5–7) and fifth (bonds 17–19) rings only show evidence of a transition region (i.e., the boundary between the quinoid and aromatic regions), in contrast to the full quinoidal character observed for the corresponding rings in the unsubstituted sexithiophene dication.

The defect confinement along the sexithiophene backbone of $(I)_2^{\bullet+/2+}$ can be seen more clearly when the changes in bond length from the neutral species are assessed [Fig. 3(c)]. The largest modifications occur in the region of the sexithiophene backbone between the positions of the styryl

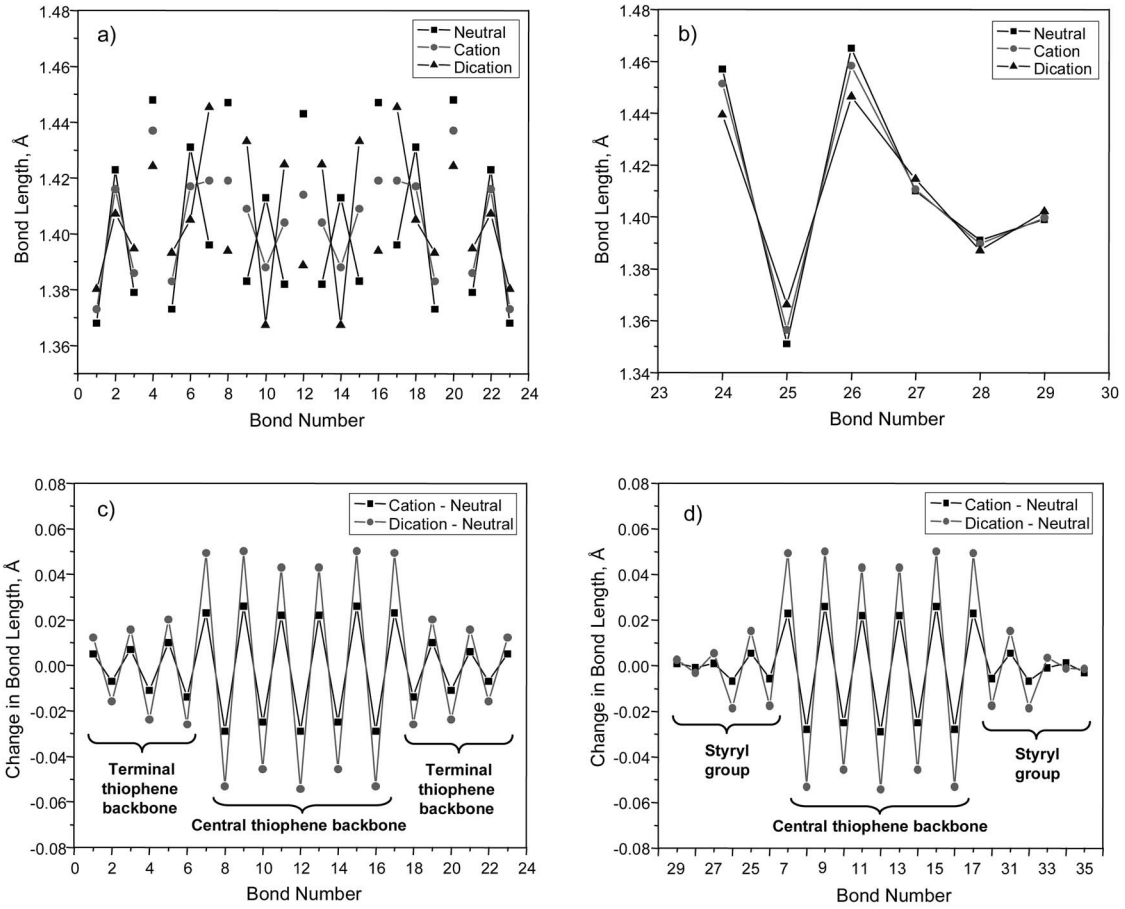

FIG. 3. The calculated [B3LYP/6-31G(*d*)] CC bond length alternation diagram for the sexithiophene backbone (a) and the styryl group (b) of $(I)_2$ and its charged species, using the bond numbering system depicted in Fig. 1. Each set of three connected symbols represents a thiophene ring, while unconnected symbols represent the inter-ring bonds. The changes in bond length along the sexithiophene backbone (c) and along the "styryl-bithiophene-styryl" conjugation path (d) between the charged and neutral species are also shown.

groups (bonds 7–17). The defect confinement is significantly more evident in the dication structure. The bond length change from neutral $(I)_2$ to $(I)_2^{2+}$ increases sharply from 0.020 Å for bond 5 to 0.049 Å for the other C_α–C_β bond in that ring, bond 7, which is the point of attachment for the styryl substituent. Within the confined central thiophene region, an average absolute bond length change of 0.049 Å is predicted for $(I)_2^{2+}$ relative to the neutral species. Much smaller bond length changes are observed at the termini: the average absolute change in bond length for the two terminal thiophene rings of $(I)_2^{2+}$ is 0.015 Å. The bond length changes from the neutral species to the dication are therefore over three times greater in the central section of the thiophene backbone than in the terminal rings.

Unsubstituted sexithiophene shows more evenly distributed bond length changes and the pronounced demarcation induced by the styryl substituents is no longer in evidence, as would be expected [Fig. 2(b)].

This phenomenon of defect confinement, seen for the dications in particular, cannot be explained by the partial extension of the structural defect into the styryl moiety. The bond length diagrams for the styryl group of $(I)_2$ and its charged species are shown in Fig. 3(b). The ethenyl bond length changes from $(I)_2$ to $(I)_2^{2+}$, averaging 0.017 Å, are very similar to that calculated for the terminal thiophene rings (0.015 Å) and are significantly smaller than the changes seen for the neighboring confined thiophene region (0.049 Å). The phenyl bond length changes are even smaller (0.004 Å). Indeed, if the conjugation path is assumed to be a "styryl-bithiophene-styryl" backbone, i.e., the central thiophene region bound by the styryl substituents and the substituents themselves, then the well-defined boundary of the confinement is still evident and in the same location [Fig. 3(d)]. The average absolute bond length change within the confined region is over 3 times that of the ethenyl moiety and 12 times that of the phenyl ring from $(I)_2$ to $(I)_2^{2+}$.

The effect of adding *R* groups to the phenyl rings was investigated. In the case of $(VII)_2$, where an electron-withdrawing cyano group has been introduced, the bond length changes from the neutral species to the dication along the sexithiophene backbone are very similar to that predicted for $(I)_2^{2+}$: the central thiophene region has an average absolute change of 0.048 Å while the terminal thiophene rings change by 0.016 Å. However, the styryl group of $(VII)_2$ shows smaller bond length changes than $(I)_2$, with the ethenyl groups averaging a change of 0.011 Å upon dication formation and the phenyl rings a negligible 0.002 Å.

A different effect is observed if the *R* substituent is an electron-donating group. The bond length alternation and bond length change diagrams for VI, which has alkoxy

TABLE I. The spin densities of the terminal α carbons and totaled over each thiophene ring (C and S atoms) and the styryl group for each sexithiophene.

	Total spin density				
Compound	Thiophene ring 1[a]	Thiophene ring 2	Thiophene ring 3[a]	Styryl group	Terminal α carbon
$6T^{\cdot+}$	0.114	0.185	0.217	⋯	0.085
$(VII)_2^{\cdot+}$	0.090	0.161	0.209	0.048	0.068
$(I)_2^{\cdot+}$	0.079	0.158	0.208	0.067	0.062
$(II)_2^{\cdot+}$	0.067	0.147	0.196	0.090	0.053
$IV^{\cdot+}$	0.060	0.137	0.182	0.112	0.048
$VI^{\cdot+}$	0.060	0.137	0.183	0.113	0.048

[a]Thiophene ring 1 indicates a terminal ring while thiophene ring 3 indicates a central ring, as shown in Fig. 1.

groups in the *meta* and *para* positions of the phenyl rings, and its charged species are shown in Fig. 1S.[25] The average absolute calculated bond length change from the neutral VI molecule to the dication for the ethenyl groups is 0.026 Å, appreciably greater than the corresponding changes seen for $(I)_2$ and $(VII)_2$ (0.017 and 0.011 Å, respectively). The phenyl rings also show larger bond length changes (0.011 Å) than the other styryl sexithiophenes (0.004 and 0.002 Å). Conversely, the absolute bond length changes observed for the central (0.045 Å) and terminal (0.011 Å) thiophene rings during the formation of VI^{2+} are slightly smaller than the other sexithiophenes [0.049 and 0.015 Å for $(I)_2$]. The electron-donating alkoxy groups therefore stabilize the charged defect and cause a weakening of the defect confinement by allowing the partial extension of the structural distortion into the styryl substituents. The electron-withdrawing–CN group in $(VII)_2$ is unable to do this and thus the defect confinement is more pronounced.

The removal of electrons leads to planarization of the oligothiophene system due to the quinoidization of the bond sequence that occurs upon oxidation.[26] The inter-ring bonds have increased electron density and are thus more rigid. The thiophene backbone dihedral angles all approach planarity to some extent. For example, dihedral angle ϕ_1 (bonds 7–9) alters from 145° in the neutral state of $(I)_2$ to 170° in the dication, despite the proximity of the styryl substituents. The central dihedral angle ϕ_2 (bonds 11–13) is almost fully planar in the dication (179°), as is ϕ_3 (bonds 3–5) (176°). The neutral species has these dihedrals at 177° and 161°, respectively. All of the compounds discussed here show the same trends. Conversely, the dihedral angles associated with the styryl substituents are predicted to change very little upon oxidation. Dihedral angle ϕ_4 (bonds 7, 24, and 25), connecting the styryl group to the sexithiophene backbone, for instance, alters by only 5° during the transition from $(I)_2$ to $(I)_2^{2+}$. The dihedral angle connecting the phenyl group to the ethenyl moiety, ϕ_5 (bonds 25–27), also hardly changes (4°).

Similar trends towards planarization were also calculated for unsubstituted sexithiophene and its charged species, as previously reported for other oligothiophenes. In the neutral species, the inter-ring dihedral angles range from 163° to 168°, while in both the radical cation and dication these reach full planarity.

Spin densities

The calculated spin densities of the sexithiophene radical cations have been summed over each thiophene ring and indicate the localization of the charged defect in the center of the oligothiophene backbone. These are shown in Table I, where "ring 1" indicates a terminal thiophene ring and "ring 3" a central ring. The calculated spin densities shown for the thiophene rings include the carbon and sulfur atoms but not the hydrogens as these have only a small spin contribution. Similarly, the spin densities indicated for the styryl groups include only the carbon atoms.

The greatest spin density is located in the central two thiophene rings and decreases to a minimum at the terminal rings. The central two rings of unsubstituted sexithiophene have a spin density a factor of 1.9 higher than the two terminal thiophene rings. Introduction of the two styryl substituents in $(I)_2^{\cdot+}$ causes this spin density difference between the central and terminal thiophene rings to increase to 2.6. This points to more strongly localized charged defects for the styryl sexithiophene and is in agreement with the results from the previous section.

Addition of one or two methoxy groups per phenyl ring [$(II)_2^{\cdot+}$, $IV^{\cdot+}$, and $VI^{\cdot+}$] causes the central thiophene rings to have a spin density three times greater than that of the terminal rings, a substantial difference compared to unsubstituted sexithiophene. However, Table I also reveals that the spin contribution of the styryl groups increases upon the addition of alkoxy groups: this compensates for the reduced spin on the terminal thiophene rings and indicates the extension of the charged defect into the styryl groups. This is again consistent with the geometry results in the previous section.

It can also be seen that the spin density on the α termini progressively decreases from the unsubstituted sexithiophene radical cation to $(I)_2^{\cdot+}$ and then the alkoxy-styryl sexithiophenes $(II)_2^{\cdot+}$, $IV^{\cdot+}$, and $VI^{\cdot+}$. This may be contributing to the enhanced stability of the alkoxy-styryl sexithiophenes radical cations and the lack of further oligomerization.[19] These effects appear to reach saturation after $IV^{\cdot+}$—there is very little difference in either the terminal α carbon spin densities or spin density distributions between this compound and $VI^{\cdot+}$.

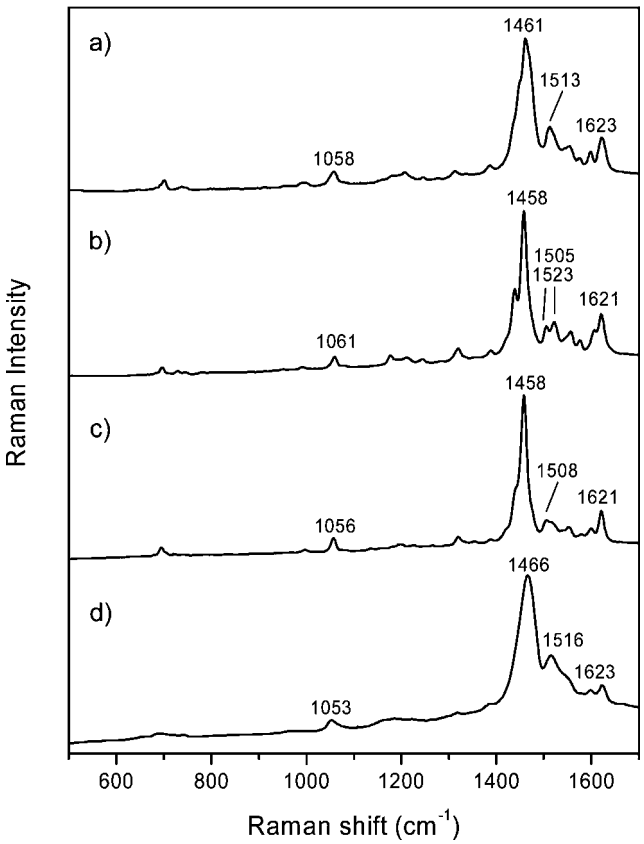

FIG. 4. Experimental solid state Raman spectra of neutral films of $(I)_2$ (a), $(II)_2$ (b), IV (c), and VI (d) using an excitation wavelength λ_{exc}=413 nm. Note that the deposition of VI was difficult and produced a poor quality film.

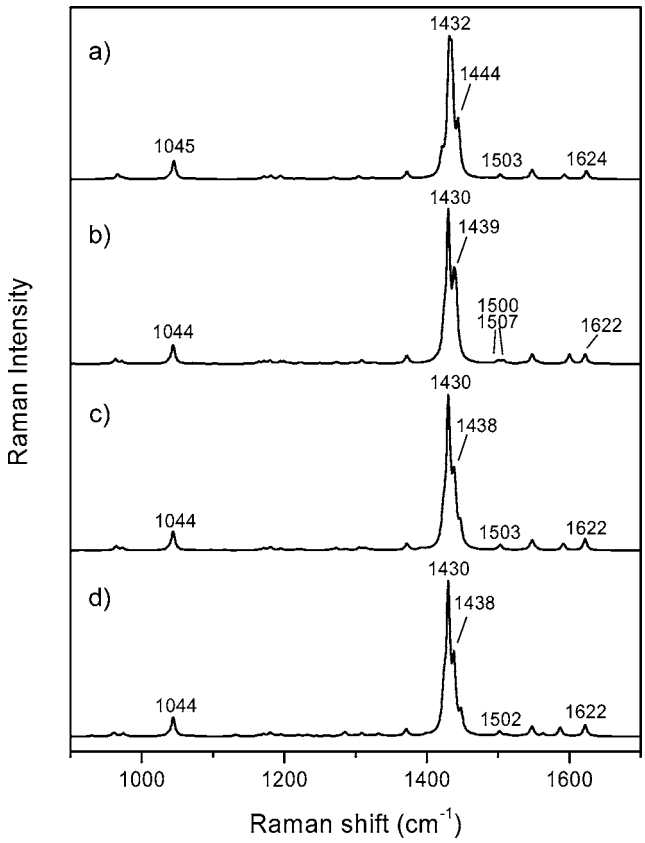

FIG. 5. Calculated [B3LYP/6-31G(*d*)] Raman spectra of neutral $(I)_2$ (a), $(II)_2$ (b), IV (c), and VI (d).

Raman spectra

Neutral monomers

The experimental solid state Raman spectra of III and V [Fig. 2S (Ref. 25)] are both very similar to those spectra measured previously for the *R*-pet series, where "pet" refers to "phenyl ethenyl terthiophene."[17] They are characterized by a number of high intensity bands in the 1440–1630 cm^{-1} region, as predicted by the theoretical calculations. These include the ethenyl and symmetrical phenyl stretches at 1630 and 1600 cm^{-1}, respectively, which are predicted at 1624 and 1588 cm^{-1}. Two asymmetrical terthiophene stretching modes are calculated at 1547 and 1523 cm^{-1} and measured at 1558 and 1527 cm^{-1} for III. The intense symmetric terthiophene stretching mode in the 1440–1450 cm^{-1} region, as seen in the *R*-pet series, is coupled to an umbrella motion of the methoxy groups in the cases of II, III, and V. This leads to an in-phase and an out-of-phase mode, which are clearly separated in the calculated Raman spectrum of V. The measured spectra show a single band correlated to these two modes at approximately 1460 cm^{-1}.

Neutral σ dimers

The Raman spectra of the neutral styryl-substituted sexithiophene films (Fig. 4) are significantly different from that of their parent monomers' spectra [Fig. 2S (Ref. 25)]. The thiophene symmetrical C═C modes in the 1430–1470 cm^{-1} region become very intense and dominate the measured spectra under both resonant and nonresonant conditions. These intense thiophene modes are also observed in the theoretical spectra (Fig. 5); however, the bands are consistently underestimated by around 30 cm^{-1}. Calculated eigenvectors for neutral $(I)_2$ of a number of important modes are shown in Fig. 3S.[25] The most intense measured band is at approximately 1460 cm^{-1} for all styryl sexithiophenes in the solid state (predicted at ~1430 cm^{-1}). This may be assigned to line *B* according to the terminology of Casado *et al.*[15] Its frequency is unaltered by the addition of the styryl groups: line *B* of unsubstituted sexithiophene is also at 1460 cm^{-1}.[6] It has been previously established that the frequency of line *B* in an oligothiophene Raman spectrum does not shift significantly with an increasing conjugation length[12] and this is observed for the compounds studied here. For example, line *B* is measured at 1458 cm^{-1} for both the monomer II and the σ-dimer $(II)_2$ and 1459 and 1455 cm^{-1} for V and VI, respectively. The relative intensity of line *B*, however, is known to increase with oligothiophene size,[27] as is observed in our styryl oligothiophene spectra [compare Figs. 1S (Ref. 25) and 4].

The asymmetrical thiophene stretches in the 1500–1550 cm^{-1} region and the higher frequency styryl modes are predicted to be relatively weak in comparison to the symmetrical thiophene modes. Line *A*, an asymmetrical thiophene stretching mode, is measured at ~1525 cm^{-1} for the neutral monomers and 1502–1516 cm^{-1} for the σ dimers, displaying the expected downshift that occurs upon an increase in conjugation length.[11,15] The σ dimerization of

V to VI shows the largest downshift of 23 cm^{-1} while the other compounds have smaller downshifts of at least 10 cm^{-1}. This may indicate that VI gains the most effective conjugation upon σ dimerization. Line *A* is predicted to occur at 1503 cm^{-1} for the styryl sexithiophenes. $(II)_2$ is interesting in that line *A* appears to have split: two very similar modes both adhering to the line *A* definition are calculated at 1500 and 1507 cm^{-1} and can be correlated to two experimental bands measured at 1505 and 1523 cm^{-1}. The sensitivity of line *A* to structure and conjugation length is apparent when the Raman spectrum is measured under different conditions. For example, line *A* is measured for VI at 1516 cm^{-1} as a film (λ_{exc}=413 nm) and 1502 cm^{-1} as a power (λ_{exc}=1064 nm). $(I)_2$ also shows this marked difference (1513 and 1505 cm^{-1}, respectively). The higher frequency observed for the film compared to the powder suggests the presence of disorder in the film.

Another mode that undergoes a downshift upon σ dimerization is the ethenyl stretch (which is combined with a weak phenyl symmetrical stretch), the highest frequency stretching mode. The downshift is smaller than that observed for line *A* at less than 10 cm^{-1} in each case. For example, the mode shifts experimentally from 1630 cm^{-1} for III to 1621 cm^{-1} for IV.

The central thiophenes' CH bending mode is another interesting feature. Similarly to line *B*, this mode gains significant intensity with an increase in conjugation length. This is observed here upon σ dimerization both theoretically and experimentally and is more apparent in the nonresonant Raman spectra (λ_{exc}=1064 nm). The mode is predicted at 1044 cm^{-1} for the styryl sexithiophenes and measured at 1056–1061 cm^{-1}. It is also observed in the Raman spectrum of unsubstituted sexithiophene but is at lower frequency (calculated at 1036 cm^{-1} and measured at 1049 cm^{-1}).

Solution state oxidized species

The Raman spectra of the styryl-substituted terthiophenes and sexithiophenes oxidized with copper perchlorate in acetonitrile solution were measured using 752 nm excitation. This excitation wavelength was used to provide resonance with the styryl sexithiophene charged species: primarily the radical cation and its π dimer, which absorb in the 805–840 and 695–750 nm ranges for these compounds, respectively (the NIR band for the styryl sexithiophenes' radical cation is located at ~1465–1580 nm in acetonitrile, while that of the π dimer is at 1170–1225 nm).[18] The sexithiophene dications have their absorption maxima at 890–985 nm but are still strongly absorbing at 752 nm.

Sexithiophene oxidation products were observed in all Raman experiments: the spectra of the oxidized monomers III and V are virtually identical to those of their σ-dimers IV and VI, respectively. Two distinct oxidation stages were measured, corresponding to the styryl sexithiophene radical cation and dication. The Raman spectrum of each oxidized species is very similar to that of the other styryl sexithiophenes. The radical cation [Figs. 6(a) and 4S (Ref. 25)] is characterized by a very intense band with its maximum at ~1434 cm^{-1}. The band is broad and thus is expected to encompass a number of modes. In the case of $(I)_2^{\cdot+}$ [Fig. 6(a)]

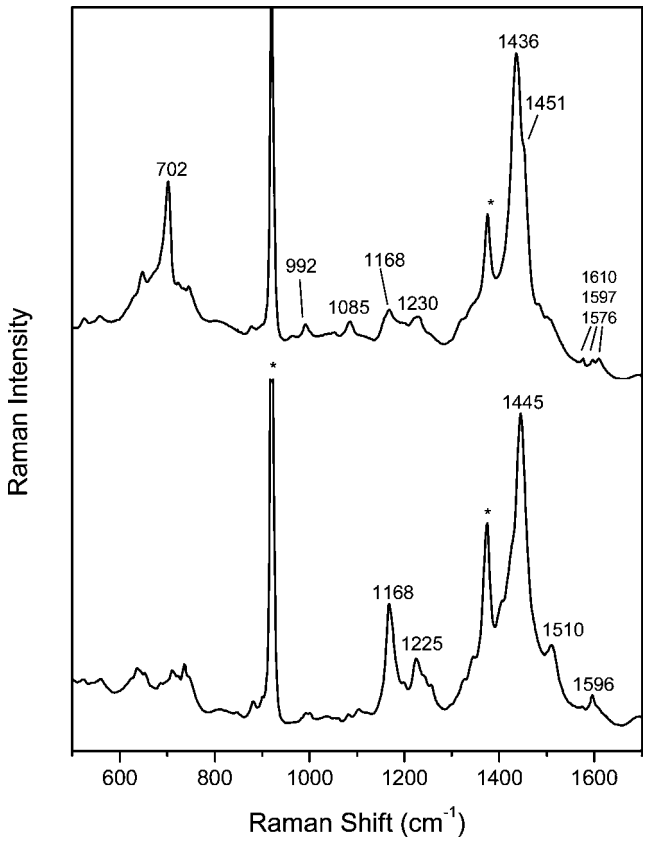

FIG. 6. Experimental solution Raman spectra of the first (a) and second (b) oxidation stages of $(I)_2$ with $Cu(ClO_4)_2$/AcN using an excitation wavelength λ_{exc}=752 nm, with an initial I concentration of 2×10^{-5} mol L^{-1}. The asterisks denote solvent bands.

one of these additional bands is evident as a shoulder at 1451 cm^{-1}. Other distinguishing features of the radical cation include a band of medium to strong intensity at 690–700 cm^{-1}, a weak band at 1085 cm^{-1}, and a group of three bands in the high frequency region of 1570–1610 cm^{-1}.

Concentrations of I over three orders of magnitude (10^{-5}–10^{-3} mol L^{-1}) were examined in order to assess the presence of any concentration dependence effects. The Raman spectrum of the radical cation $(I)_2^{\cdot+}$ was identical in terms of frequencies and relative intensities for each concentration. The level of π dimerization increases with concentration, thus at higher concentration levels the π-dimer species predominate.[18] The fact that there is no change in the spectrum points to π-dimer formation which does not greatly perturb the vibrational spectrum; that is the vibrational spectrum of isolated $(I)_2^{\cdot+}$ and the corresponding π-dimer species are similar. Thus in this case it is valid to compare the experimental data, which is likely to be mainly π-dimer species, to that calculated for isolated $(I)_2^{\cdot+}$. Clearly if a stronger interaction did exist and the spectra varied with concentration then calculations of the π dimer would be essential to model the system.

The calculated Raman spectra of the styryl sexithiophene radical cations [Figs. 7(a) and 5S (Ref. 25)] share a number of similar features. They all possess a single very intense band located at 1377–1392 cm^{-1}, showing a

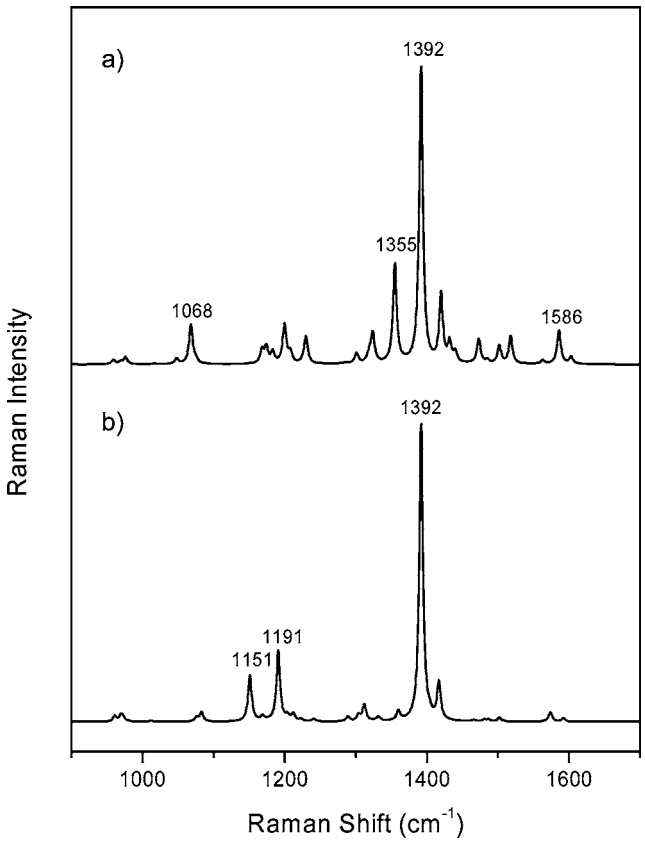

FIG. 7. Calculated [B3LYP/6-31G(*d*)] Raman spectra of the $(I)_2$ radical cation (a) and dication (b).

consistent downshift from $(I)_2^{\bullet+}$ to $VI^{\bullet+}$ with an increasing alkoxy substitution. This band belongs to a symmetrical CC stretching mode that is strongly localized on the two central thiophenes' inter-ring bonds. The eigenvector of this $(I)_2^{\bullet+}$ mode is shown in Fig. 8(a). In the case of those molecules with alkoxy groups, this mode also has some contribution from the styryl groups. It is probable that this calculated band can be correlated with the very intense experimental band at $\sim$1434 cm^{-1}. An appreciably smaller downshift of only 3 cm^{-1} is observed experimentally from $(I)_2^{\bullet+}$ to $VI^{\bullet+}$ in comparison to that predicted (15 cm^{-1}). Some caution must be exercised in comparing calculated Raman intensities with those observed in resonance Raman spectra, as the resonance enhancement effect is mode dependent. Nonetheless the resonance Raman spectra observed arise from *A*-term scattering and this enhancement mechanism favors totally symmetric modes. Thus the assignment of the strong band at $\sim$1434 cm^{-1} to a calculated totally symmetric mode is consistent. As was observed for the neutral σ dimers, the position of the measured band is not well reproduced by the calculation; this is especially apparent for the alkoxy-substituted compounds.

Another important calculated band characteristic of the radical cation is the CH bending mode localized on the central two thiophene rings [Fig. 8(b)]. It is predicted at 1068 cm^{-1} and correlated to the measured band at 1085 cm^{-1} for $(I)_2^{\bullet+}$. This mode has upshifted significantly from its position in the experimental neutral σ-dimer spectrum, 1056 cm^{-1} (calculated at 1044 cm^{-1}).

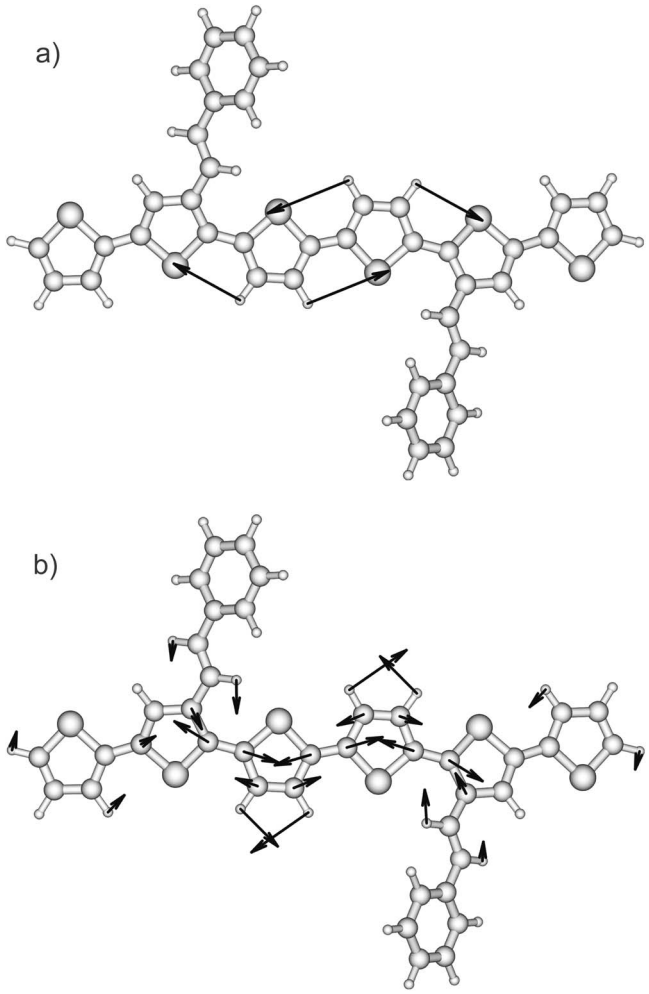

FIG. 8. The eigenvectors of selected pertinent calculated modes of the $(I)_2$ radical cation: 1068 (a) and 1392 (b) cm^{-1}.

The group of three bands in the 1570–1610 cm^{-1} region of the experimental radical cation spectra can be assigned to styryl localized stretching modes. The highest frequency mode, which is mostly localized on the ethenyl unit, is measured at 1610 cm^{-1} in the case of $(I)_2^{\bullet+}$ and has downshifted from its corresponding mode in the Raman spectrum of the neutral species (1623 cm^{-1}). This change has been also observed in the theoretical spectra (with a downshift from 1624 to 1603 cm^{-1} predicted) and is caused by the loss of double bond character in the ethenyl bond upon quinoidization in the radical cation. In turn, this indicates that the polaronic defect has slightly extended into the styryl substituents, as discussed in the previous section.

This effect is very noticeable in the Raman spectra recorded during the oxidation of VII, where the neutral band at 1626 cm^{-1} decaying while the radical cation band at 1615 cm^{-1} grows is observable on the time scale of the experiment. This ethenyl stretching mode is of higher frequency in $(VII)_2^{\bullet+}$ than in the other styryl sexithiophene radical cations, as predicted. Indeed, $(VII)_2^{\bullet+}$ possesses a slightly different solution spectrum to that of the other radical cations [Fig. 6S (Ref. 25)]. In particular, the highest intensity band is located at lower frequency (1422 cm^{-1}), the central thiophenes' CH bending mode is upshifted to 1090 cm^{-1}, and

instead of three clustered bands in the high frequency region, there are only two (1600 and 1614 cm^{-1}). The lower frequency of the strongest band will be addressed later.

The Raman spectra of the radical cation and dication of unsubstituted sexithiophene, 6T, were also measured for comparison purposes. These spectra were identical to those measured by Yokonuma *et al.* in dichloromethane using iron chloride.[28] The Raman spectrum of $6T^{\cdot+}$ has the same pattern as the styryl sexithiophene radical cations, with the most intense band located at 1440 cm^{-1}. The thiophene CH bending modes at 1067 and 1055 cm^{-1} are downshifted from that of the styryl sexithiophenes' (1085 cm^{-1}). Two other modes seen clearly in the Raman spectrum of $(I)_2^{\cdot+}$ at 1168 and 1230 cm^{-1} have their counterparts in the $6T^{\cdot+}$ spectrum at 1160 and 1234 cm^{-1}. A group of intense bands was also measured in the 650–700 cm^{-1} region for $6T^{\cdot+}$, similar to that observed for $(I)_2^{\cdot+}$ and $(II)_2^{\cdot+}$, in particular.

Other sexithiophene radical cation Raman spectra have been measured by Casado *et al.*, including dimethyl end-capped sexithiophene (DM6T).[7] This radical cation spectrum is dominated by a very intense band at 1438 cm^{-1}, again at a very similar position to that of unsubstituted 6T and the styryl sexithiophenes. Also observed were bands of medium intensity at 1217, 1164, and 1049 cm^{-1}, also comparable to the other radical cation spectra. Other sexithiophene radical cation Raman spectra, such as dihexyl end-capped sexithiophene[2] and biphenyl end-capped sexithiophene with butyl solubilizing side chains,[8] have also been measured.

Further oxidation induces additional changes to the Raman spectra of the styryl sexithiophenes. This second oxidation stage corresponds to the formation of the dication species and is characterized by the most intense band shifting slightly upwards in frequency to 1441–1445 cm^{-1} [Fig. 6(b) and 4S (Ref. 25)], a change of only 8–9 cm^{-1}. Other distinctive features of the dication spectrum include an intense band at ~1165 cm^{-1}, along with the disappearance of the high frequency cluster of three bands and, in the case of $(I)_2^{2+}$, the loss of the intense 702 cm^{-1} band. The 1085 cm^{-1} band loses much of its intensity but is still evident in several of the dication spectra, indicating the continued (but decreased) presence of radical cation.

In general, it is expected that the most intense band in an oligothiophene Raman spectrum, usually a strong C=C symmetrical stretch of the thiophene backbone, should progressively downshift in frequency from the neutral molecule to the charged species. This occurs as the quinoidal nature of the backbone increases during the oxidation process and the double bond character of the C=C bonds is reduced. This has been observed during the oxidations of various oligothiophenes.[29] For example, the strong band in the DM6T Raman spectrum at 1477 cm^{-1} (Ref. 3) downshifts to 1438 cm^{-1} in the radical cation then to 1417 cm^{-1} in the dication.[16]

However, this trend is not observed here for the formation of the styryl sexithiophene dication $(I)_2^{2+}$ from the radical cation. Instead, a small upshift occurs, from 1436 to 1445 cm^{-1}. The calculated Raman spectrum of $(I)_2^{2+}$ [Fig. 7(b)] has a single very intense band at 1392 cm^{-1}, the same position as the strongest band in the calculated radical cation spectrum. These two intense calculated bands of the radical cation and dication both belong to an identical vibrational mode, a symmetrical C–C stretching mode localized on the two central thiophenes' inter-ring bonds [Figs. 8(a) and 7S (Ref. 25)]. It would therefore be expected that the formation of the dication from the radical cation would further increase the double bond character of these inter-ring bonds, leading to the frequency upshift that is observed in the corresponding experimental bands. Eigenvectors of the important $(I)_2^{2+}$ modes are shown in Fig. 7S.[25]

It is also interesting to note that the eigenvector of this intense mode is localized within the confined region of the charged defect. The unusual small upshift seen during the transition between the radical cation and dication, rather than the usual sizable downshift, could therefore be seen as an indication that the proposed defect confinement is indeed occurring experimentally in these styryl sexithiophene charged species, particularly in case of the dications.

The calculated Raman spectrum of $(I)_2^{2+}$ provides a number of other correlations with the experimental spectra. Two bands of medium intensity are predicted at 1151 and 1191 cm^{-1} and can be assigned to the two measured bands at 1168 and 1225 cm^{-1}. Both these modes are due to C–S stretches localized on the central two thiophene rings. The 1068 cm^{-1} band (also localized on the central two thiophenes) predicted for the radical cation upshifts to 1083 cm^{-1} in the dication and loses most of its intensity. This is observed experimentally as the measured band at 1085 cm^{-1} decays and a very weak band at 1105 cm^{-1} appears.

The calculated Raman spectra of the other styryl sexithiophene dications [Fig. 5S (Ref. 25)] show a consistent downshift of the most intense band with an increasing alkoxy substitution, as was the case with the radical cations. The band shifts from 1392 cm^{-1} for $(I)_2^{2+}$ to 1360 cm^{-1} for IV^{2+} and VI^{2+}, a predicted downshift approximately twice that seen for the radical cation. In addition, although there is no shift predicted for the calculated intense 1392 cm^{-1} Raman band of the $(I)_2^{\cdot+} \rightarrow (I)_2^{2+}$ transition, a downshift of 17 cm^{-1} is predicted for the $VI^{\cdot+} \rightarrow VI^{2+}$ transition. This downshift is not observed experimentally: the Raman spectra of all the alkoxy-substituted styryl sexithiophene charged species strongly resemble that of the unsubstituted styryl sexithiophene $(I)_2$ in terms of band positions and intensities and the trends observed upon oxidation. The lack of correspondence with the predicted downshifts upon alkoxy substitution suggests that the calculations have overestimated the electronic effects of the alkoxy groups. The structural changes induced by the oxidation process are therefore strongly dominated by the styryl sexithiophene backbone and the alkoxy substituents contribute little.

The solution Raman spectra of the styryl sexithiophene radical cations and dications were measured at a variety of other excitation wavelengths, $\lambda_{exc}=568-1064$ nm to check for any significant intensity changes. Higher energy wavelengths could not provide any useful information due to interference from fluorescence. The dication spectra were most easily obtainable at $\lambda_{exc}=1064$ nm, where the absorption band of this species occurs. The same relative intensity pat-

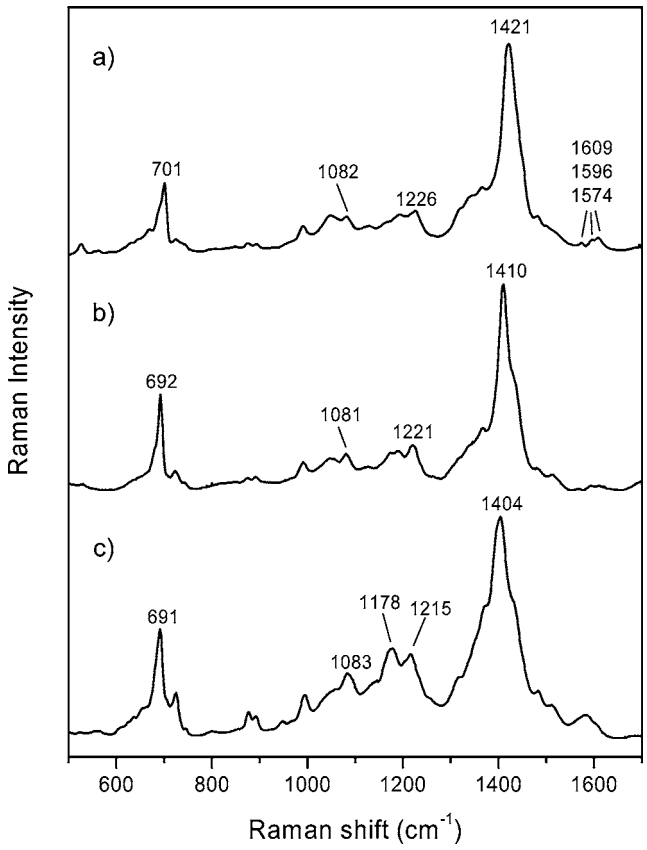

FIG. 9. Experimental solid state Raman spectra of oxidized films of $(I)_2$ (a), $(II)_2$ (b), and VI (c) using an excitation wavelength $\lambda_{exc}=752$ nm.

tern for the charged species was measured at each wavelength. This suggests that the comparison of intensities between the experimental and the theoretical spectra of the $(I)_2$ charged species has validity.

Solid state oxidized species

It has been previously established that the Raman spectra of thiophenes are dependent upon state. For instance, the strongest band of neutral polyhexylthiophene was measured at 1475 cm^{-1} in solution and 1448 cm^{-1} as a solid.[30] This has been attributed to the increase in effective conjugation length that occurs as a result of planarization in the solid.

The Raman spectra of electrochemically oxidized films (Fig. 9) were therefore measured using 752 nm excitation for comparison with the solution state spectra. Despite using a range of oxidation potentials and deposition times, evidence of solely radical cations was found for each compound; no dication features were present in any of the spectra. The higher stability of the styryl sexithiophene radical cations compared to the dications has been previously established.[18] It is likely that the presence of favorable π stacking of radical cations in the solid state[31] further enhances their stability over that of the dications, leading to their predominance in the oxidized species spectra. Films (both reduced and oxidized) were difficult to generate for compounds IV and VI due to their higher solubilities and very long deposition times were required.

The Raman spectrum of solid oxidized $(I)_2$ is virtually identical to the solution state radical cation spectrum, with the group of three bands in the 1570–1610 cm^{-1} region, the 1082 cm^{-1} CH bending mode, and the intense 701 cm^{-1} band. The only significant difference is in the frequency of the strongest band, which is located at 1436 cm^{-1} in solution but downshifted to 1421 cm^{-1} in the film. This also occurs for the alkoxy-substituted styryl sexithiophenes, but the effect becomes increasingly exacerbated along the compound series: $(II)_2^{\cdot+}$ undergoes a downshift of 25 cm^{-1} and $VI^{\cdot+}$ 32 cm^{-1}. In comparison, the unsubstituted sexithiophene radical cation shows a downshift of 14 cm^{-1} between the solution and solid states.

$(VII)_2^{\cdot+}$, however, displays a negligible downshift between the solution and solid states of only 3 cm^{-1} for this mode [Fig. 6S (Ref. 25)]. As discussed previously, the solution state spectrum of $(VII)_2^{\cdot+}$ shows this band to already be appreciably downshifted from the other styryl sexithiophenes (1422 cm^{-1} as opposed to ~1434 cm^{-1}). It is likely that this is due to the lack of solubility of the $(VII)_2$ charged species, which can be seen to form a dark precipitate upon oxidation. The Raman spectrum of the precipitate is therefore closer to that observed for the solid state spectrum rather than a solution state spectrum.

The downshifts of this intense symmetrical CC mode from the solution to the solid state in the other styryl sexithiophene radical cations are quite large; in fact, they are greater than that observed for the corresponding neutral species. Neutral VI, for instance, shows a downshift of its strongest band of only 6 cm^{-1} between the solution and solid states. This suggests that the increase in effective conjugation length is greater for the radical cations than for the neutral species. A possible explanation for this behavior is that the radical cation forms π stacks in the solid film and the resultant intermolecular interactions effectively allow a further extension of the electron delocalization and therefore the conjugation,[31] particularly for those compounds with alkoxy substituents on the phenyl rings.

CONCLUSIONS

The calculated geometries of the styryl sexithiophene charged species indicate a quinoidal structural defect that is more strongly localized than in other sexithiophenes. The charged defect appears to be confined by the positions of the styryl substituents. This defect confinement is particularly apparent in the dication but begins to weaken in the alkoxy-substituted styryl sexithiophenes due to the structural defect extending into the styryl groups, a result of the electron-donating character of the alkoxy moieties.

In addition, the calculated spin densities of the styryl sexithiophene radical cations show an appreciably larger difference in spin between the central and terminal rings than is observed for unsubstituted sexithiophene. The weakening of the defect confinement in the alkoxy-styryl sexithiophenes is manifested by a large spin contribution from the styryl substituents.

The experimental Raman spectra of the neutral styryl sexithiophenes are characterized by very intense thiophene backbone symmetrical stretching modes, which are also evident in the theoretical spectra. The solution state spectra of

the oxidized species reveal two oxidation stages: the radical cation and dication. Rather than the expected downshift of the intense thiophene stretching mode from the radical cation to the dication, a small upshift is observed. The eigenvector for this mode reveals that it is localized over the same area occupied by the confined defect.

The solid state Raman spectra of electrochemically oxidized films show evidence of radical cations only. It is probable that their enhanced stability (compared to dications) in the solid state, due to π stacking, is contributing to this phenomenon. The Raman spectra show downshifts of the intense thiophene stretching mode from the corresponding mode in the solution spectra. The magnitude of the shift is dependent upon the substitution on the styryl group and can be quite large ($\sim 30\ \mathrm{cm}^{-1}$), possibly indicating an extension of the conjugation via intermolecular interactions.

This study reveals that the charged defects created by radical cation and dication formation are structurally very dependent upon the substitution along the thiophene backbone. In the case of these styryl-substituted sexithiophenes, the defect is strongly confined within the central portion of the thiophene chain, which explains the low reactivity of these systems towards polymerization. Solid samples show greater conjugation in the oxidized state: such factors would have a strong bearing on the behavior of electronic devices such as field-effect transistors (FETs) and organic light-emitting diodes (OLEDs) fabricated from these compounds.

ACKNOWLEDGMENT

The authors are grateful to the New Zealand Foundation of Science, Research and Technology and the University of Otago for support.

[1] A. Pron and P. Rannou, Prog. Polym. Sci. **27**, 135 (2001); W. A. Gazotti, A. F. Nogueira, E. M. Girotto, L. Micaroni, M. Martini, S. das Neves, and M. A. De Paol, *Handbook of Advanced Electronic and Photonic Materials and Devices* (Academic Press, San Diego, 2001), Vol. 10, p. 53.
[2] J. Casado, H. E. Katz, V. Hernandez, and J. T. Lopez Navarrete, J. Phys. Chem. B **106**, 2488 (2002).
[3] V. Hernandez, J. Casado, F. J. Ramirez, G. Zotti, S. Hotta, and J. T. L. Navarrete, J. Chem. Phys. **104**, 9271 (1996).
[4] J. Casado, L. L. Miller, K. R. Mann, T. M. Pappenfus, Y. Kanemitsu, E. Orti, P. M. Viruela, R. Pou-Amerigo, V. Hernandez, and J. T. Lopez Navarrete, J. Phys. Chem. B **106**, 3872 (2002).
[5] F. Garnier, G. Horowitz, X. Peng, and D. Fichou, Adv. Mater. (Weinheim, Ger.) **2**, 592 (1990); G. Horowitz, F. Garnier, A. Yassar, R. Hajlaoui, and F. Kouki, *ibid.* **8**, 52 (1996); F. Garnier, Chem. Phys. **227**, 253 (1998); D. Fichou, P. Demanze, G. Horowitz, R. Hajlaoui, M. Constant, and F. Garnier, Synth. Met. **85**, 1309 (1997); R. Hajlaoui, G. Horowitz, F. Garnier, A. Arce-Brouchet, L. Laigre, A. El Kassmi, F. Demanze, and F. Kouki, Adv. Mater. (Weinheim, Ger.) **9**, 389 (1997).
[6] Y. Furukawa, J. Phys. Chem. **100**, 15644 (1996).
[7] J. Casado, V. Hernandez, S. Hotta, and J. T. Lopez Navarrete, J. Chem. Phys. **109**, 10419 (1998).
[8] J. Casado, L. L. Miller, K. R. Mann, T. M. Pappenfus, V. Hernandez, and J. T. Lopez Navarrete, J. Phys. Chem. B **106**, 3597 (2002).
[9] J. Cornil, D. Beljonne, and J. L. Bredas, J. Chem. Phys. **103**, 842 (1995).
[10] C. Ehrendorfer and A. Karpfen, J. Phys. Chem. **98**, 7492 (1994).
[11] V. Hernandez, J. Casado, and J. T. Lopez Navarrete, J. Mol. Struct. **521**, 249 (2000).
[12] C. Moreno Castro, M. C. Ruiz Delgado, V. Hernandez, S. Hotta, J. Casado, and J. T. Lopez Navarrete, J. Chem. Phys. **116**, 10419 (2002).
[13] V. Hernandez, J. Casado, F. Effenberger, and J. T. Lopez Navarrete, J. Chem. Phys. **112**, 5105 (2000).
[14] J. Casado, J. J. Maraver Puig, V. Hernandez, G. Zotti, and J. T. Lopez Navarrete, J. Phys. Chem. A **104**, 10656 (2000); V. Hernandez, J. Casado, Y. Kanemitsu, and J. T. Lopez Navarrete, J. Chem. Phys. **110**, 6907 (1999); J. Casado, V. Hernandez, Y. Kanemitsu, and J. T. L. Navarrete, J. Raman Spectrosc. **31**, 565 (2000).
[15] J. Casado, S. Hotta, V. Hernandez, and J. T. Lopez Navarrete, J. Phys. Chem. A **103**, 816 (1999).
[16] J. Casado, V. Hernandez, S. Hotta, and J. T. Lopez Navarrete, Adv. Mater. (Weinheim, Ger.) **10**, 1458 (1998).
[17] T. M. Clarke, K. C. Gordon, D. L. Officer, S. B. Hall, G. E. Collis, and A. K. Burrell, J. Phys. Chem. A **107**, 11505 (2003).
[18] T. M. Clarke, K. C. Gordon, D. L. Officer, and D. K. Grant, J. Phys. Chem. A **109**, 1961 (2005).
[19] D. K. Grant, K. W. Jolley, D. L. Officer, K. C. Gordon, and T. M. Clarke, Org. Biomol. Chem. **3**, 2008 (2005).
[20] G. E. Collis, A. K. Burrell, S. M. Scott, and D. L. Officer, J. Org. Chem. **68**, 8974 (2003).
[21] S. L. Howell and K. C. Gordon, J. Phys. Chem. A **108**, 2536 (2004).
[22] G. W. T. M. J. Frisch, H. B. Schlegel, G. E. Scuseria *et al.*, GAUSSIAN 03, Gaussian, Inc., Pittsburgh, PA, 2003.
[23] A. P. Scott and L. Radom, J. Phys. Chem. **100**, 16502 (1996).
[24] J. Casado, H. E. Katz, V. Hernandez, and J. T. Lopez Navarrete, Vib. Spectrosc. **30**, 175 (2002).
[25] See EPAPS Document No. E-JCPSA6-124-507613 for the bond length alternation and change in bond length diagrams for the VI system (Fig. 1S), the theoretical and experimental Raman spectra of III and V (Fig. 2S), the eigenvectors of particular vibrational modes of neutral I_2 (Fig. 3S), the experimental solution spectra of oxidized VI (Fig. 4S), calculated Raman spectra of VI^{*+} and VI^{2+} (Fig. 5S), the neutral and oxidized solution state and solid state Raman spectra of VII (Fig. 6S), and the eigenvectors of particular vibrational modes of $(I)_2^{2+}$ (Fig. 7S). This document can be reached via a direct link in the online article's HTML reference section or via the EPAPS homepage (http://www.aip.org/pubservs/epaps.html).
[26] T. Nishinaga, A. Wakamiya, D. Yamazaki, and K. Komatsu, J. Am. Chem. Soc. **126**, 3163 (2004).
[27] E. Agosti, M. Rivola, V. Hernandez, M. Del Zoppo, and G. Zerbi, Synth. Met. **100**, 101 (1999).
[28] N. Yokonuma, Y. Furukawa, M. Tasumi, M. Kuroda, and J. Nakayama, Chem. Phys. Lett. **255**, 431 (1996).
[29] J. Casado, M. C. Ruiz Delgado, Y. Shirota, V. Hernandez, and J. T. Lopez Navarrete, J. Phys. Chem. B **107**, 2637 (2003); J. Casado, V. Hernandez, S. Hotta, and J. T. Lopez Navarrete, Synth. Met. **119**, 305 (2001).
[30] G. Zerbi, B. Chierichetti, and O. Ingaenas, J. Chem. Phys. **94**, 4646 (1991).
[31] D. D. Graf, R. G. Duan, J. P. Campbell, L. L. Miller, and K. R. Mann, J. Am. Chem. Soc. **119**, 5888 (1997).